Electrochimica Acta 385 (2021) 138428

Contents lists available at ScienceDirect

Electrochimica Acta

journal homepage: www.elsevier.com/locate/electacta

A limiting current sensor based on porous Ni electrode for ferricyanide and ferrocyanide detection in aqueous solutions

Pengcheng Zhu[1,*], Yuyuan Zhao

School of Engineering, University of Liverpool, Liverpool L69 3GH, UK

ARTICLE INFO

Article history:
Received 9 December 2020
Revised 8 April 2021
Accepted 18 April 2021
Available online 26 April 2021

Keywords:
Electrochemical detection
Limiting current sensor
Porous electrode
Ferricyanide
Ferrocyanide

ABSTRACT

The pursuit of better electrochemical sensors highlights the requirements for new sensor designs and electrode materials. The concept of 'limiting current sensor' has been validated but confined in gas detection. Herein, we applied the concept of 'limiting current sensor' to ions detection in aqueous solutions. A limiting current sensor prototype has been developed for the detection of two potentially hazardous ions, ferricyanide and ferrocyanide, which are widely used in nuclear wastewater treatment, food production and energy generation. The limiting current sensor consists of a three-electrode electrochemical cell equipped with a porous Ni working electrode and a pumping system. The pumping system forces the solution containing ferricyanide/ferrocyanide to flow through the porous Ni electrode, markedly increasing the mass transfer rate. The enhanced mass transfer rate, together with the high surface area of the porous Ni working electrode, increases the reaction rate and in turn improves the detection performance. The limiting current sensor shows two orders of magnitude higher sensitivity and one order of magnitude lower limit of detection than previously reported sensors and exhibits excellent thermal stability, long-term stability and selectivity. The limiting current sensor design can be extended to the detection of other ions or molecules.

1. Introduction

Electrochemical sensors have been widely used for detection of ions or molecules in aqueous solutions due to many unique advantages, such as simplicity, cost-effectiveness, high sensitivity, easy of miniaturization, reliability, and reproducibility [1,2]. The detection performance of electrochemical sensors is heavily influenced by electrode material and sensor design. The recent development of electrode materials, e.g. various nanostructured metals, oxides, graphene and organic materials [3–5], greatly advances the detection performance of electrochemical sensors. These electrodes normally have high surface area and electrical conductivity, which are beneficial for increasing reaction rates and in turn detection performance, e.g. sensitivity and limit of detection (LOD). Moreover, many efforts have been made in optimising the design or adopting different electrochemical techniques, e.g. potentiostatic techniques, galvanostatic techniques, potentiometery, impedance measurement and electrochemiluminescence [6,7] to achieve better detection performance.

'Limiting current sensor' is an established concept which has been extensively used for oxygen detection [8–10]. A typical limiting current oxygen sensor consists of a diffusion barrier, solid electrolyte (normally yttria-stabilized zirconia, YSZ) between two porous Pt electrodes. An external circuit is connected to the two Pt electrodes to apply voltage [11]. Heaters are employed to maintain a high working temperature. Under the working condition, the gas sample containing oxygen diffuses through the diffusion barrier and reduces to oxygen ions on one Pt electrode. The oxygen ion can transport through the YSZ solid electrolyte and then oxidise to gaseous oxygen on the other Pt electrode. In a specific applied potential range, the reaction current is constant and limited by the diffusion rate of oxygen, known as limiting current. The limiting current is proportional to the oxygen concentration and therefore can be used as a signal for oxygen detection. The concept of 'limiting current sensor' is merely used in gas detection and has not been used for detection of ions in aqueous solutions.

Ferricyanide, $Fe(CN)_6^{3-}$, is a commonly used ion in cyanotype photographing and blueprint drawing [12]. Ferrocyanide, $Fe(CN)_6^{4-}$, serves as an anticaking agent in salt production as well as a precipitant for the removal of radio-caesium from nuclear waste solutions [13,14]. The redox system between ferricyanide and ferrocyanide has also been proposed to be used in redox flow batteries [15]. Ferricyanide and ferrocyanide are po-

* Corresponding author.
E-mail addresses: p.zhu@bham.ac.uk (P. Zhu), Y.Y.Zhao@liverpool.ac.uk (Y. Zhao).
[1] Present address: School of Chemistry, University of Birmingham, Edgbaston, Birmingham B15 2TT, UK

https://doi.org/10.1016/j.electacta.2021.138428
0013-4686/

tentially hazardous to the human body because both ferricyanide and ferrocyanide can release highly toxic gaseous cyanide at high temperatures or with the addition of acids [16]. Therefore, it is necessary to precisely monitor the level of ferricyanide and ferrocyanide.

Conventional electrochemical sensors are normally made by three-electrode electrochemical cells, which measure the concentration of ferricyanide/ferrocyanide in stationary aqueous electrolytes [17–19]. Analytes diffuse towards and oxidise/reduce on the surface of a working electrode, generating an anodic/cathodic peak current. The concentration of analytes can be calculated from the peak current based on the proportional correlation between peak current and concentration of analytes. Spectroelectrochemical sensor is an alternative for ferricyanide/ferrocyanide detection. Analytes oxidise or reduce on the surface of an optically transparent electrode. An incident beam passes through the transparent electrode during the reaction and the transmitted beam is monitored. The change between the incident and transmitted beams directly results from the disappearance of analytes or appearance of reaction products [20–23]. The concentration of ferricyanide and ferrocyanide can therefore be determined by the light absorbence of the transparent electrode. Nevertheless, the complex configuration is a major limitation for the spectroelectrochemical sensor. Besides, neither conventional electrochemical sensors nor spectroelectrochemical sensors can provide satisfying performance. For example, the highest amperometric sensitivity is 0.02 mA/mM from conventional electrochemical sensors [24] and the lowest achievable LOD is 8 μM from spectroelectrochemical sensors [21]. This highlights the need for the development of better sensors.

In this paper, we developed a limiting current sensor for detection of ferricyanide and ferrocyanide ions. To the best of our knowledge, this is the first attempt to apply the limiting current concept for ion detection in aqueous solutions. The limiting current sensor consists of a three-electrode electrochemical cell and a pumping system. The working electrode is a porous Ni manufactured by a powder metallurgy method with high fluid permeability and surface area [25]. The limiting current sensor exhibits detection sensitivities two orders of magnitude higher and LODs one order of magnitude lower than previously reported sensors. We also compared the limiting current sensor with a typical conventional electrochemical sensor using the same porous Ni working electrode. The effect of fluid flow rate on the sensing performance was investigated. The thermal stability, long-term stability and selectivity of the limiting current sensor were tested. This work not only develops a limiting current sensor prototype for sensing ferricyanide and ferrocyanide, but also provides a novel design route of electrochemical sensors for other ions and molecules.

2. Methods

2.1. Preparation of porous Ni

A porous Ni sample with a porosity of 0.7 and a pore size of 425–710 μm was manufactured by the Lost Carbonate Sintering (LCS) process [25]. Pure Ni powder with a mean particle size of 45 μm was first mixed with rounded K_2CO_3 particles with a size range of 425–710 μm, at a volume ratio of 3:7. The mixture was compacted at a pressure of 200 MPa and sintered at 950 °C for 2 h. The Ni particles were sintered together and K_2CO_3 particles were removed by decomposition during sintering. The obtained sample was subsequently cut into a cylindrical shape with a diameter of 6 mm and a height of 5 mm. The porous nickel sample was washed by 10% HCl solution to remove oxides on the surface and then rinsed in distilled water before use.

2.2. Fluid permeability measurement

The fluid permeability of the porous sample was measured in a purpose-built apparatus, as detailed in [26]. The fluid permeability, K (m^2), of the porous sample was determined using the Forchheimer equation [27]:

$$\frac{\Delta P}{L} = \frac{\mu}{K}V + \rho C V^2 \quad (1)$$

where ΔP is the difference between the inlet and outlet water pressures (Pa), L is the length of the porous sample (m), μ is the viscosity of water (8.9×10^{-4} Pa s), ρ is the density of water (997 kg/m^3) and V is the Darcian velocity (m/s), which is the volumetric flow rate divided by the cross-sectional area of the porous sample.

2.3. Surface area measurement

The Brunauer–Emmett–Teller (BET) surface area measurement was conducted in a 3-Flex 3500 gas sorption analyser at 77 K using the nitrogen adsorption method. The porous Ni sample was degassed at 300°C under vacuum for 3 h before the measurement.

2.4. Electrochemical characterisation

Electrochemical characterisation of the LCS porous Ni was performed by a three-electrode electrochemical cell with a saturated calomel electrode (SCE) reference electrode, a platinum coil counter electrode in 0.1 M KOH electrolyte. Double layer capacitance test was conducted in a potential range from -0.3 to -0.2 V, at a scan rate of 0.5 V/s. Electrochemical impedance was tested from 100 kHz to 0.1 Hz.

2.5. Conventional electrochemical sensor

A conventional electrochemical sensor, consisting of a porous Ni working electrode, a SCE reference electrode and a platinum coil counter electrode, was built to measure the ferricyanide and ferrocyanide concentrations. 0.1 M KOH was used as the background electrolyte. The cyclic voltammetry technique was employed, with the applied potential starting from 0.4 to -0.2 V and from -0.2 to 0.4 V for the determinations of ferricyanide and ferrocyanide concentrations, respectively, at four different scan rates of 0.005, 0.01, 0.05 and 0.1 V/s. The redox reaction between ferricyanide and ferrocyanide in the applied potential range is expressed by Eq. (2) [28].

$$[Fe(CN)_6]^{3-} + e^- \leftrightarrow [Fe(CN)_6]^{4-} \quad (2)$$

The anodic peak current at a potential around 0.25 V was used to determine the concentrations of ferricyanide and ferrocyanide. The detection sensitivity was determined as the change in the peak current divided by the change in concentration [29]. The limit of detection (LOD) was determined according to signal/noise=3 [30], for facilitating comparison with other sensors:

$$LOD = 3.3\frac{\sigma}{S} \quad (3)$$

where σ is the residual standard deviation of the regression line and S is the slope of the regression line.

2.6. Limiting current sensor

Fig. 1 shows a schematic diagram of the limiting current sensor. The sensor contains a pumping system and a three-electrode electrochemical cell. The pump is connected to the porous Ni sample using an acrylic tube. A solution containing ferricyanide/ferrocyanide was forced to pass through the porous Ni

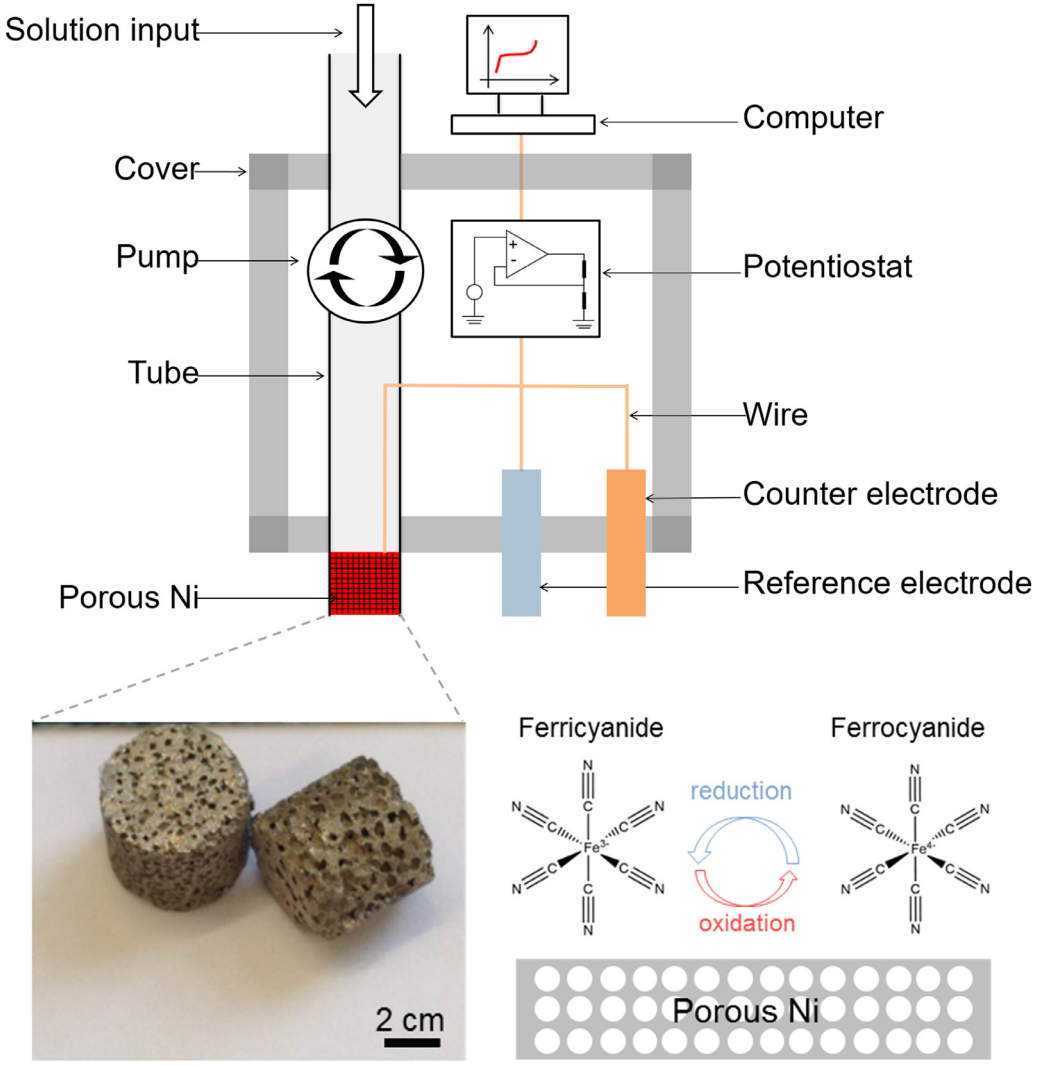

Fig. 1. Schematic illustration of the limiting current sensor for the detection of ferricyanide and ferrocyanide; the bottom-left graph shows the macrograph of two porous Ni electrodes; the bottom-right graph illustrates the redox reaction between ferricyanide and ferrocyanide on the surface of the porous Ni electrode.

sample at different flow rates of 16.8, 42 and 84 mL/min. The three-electrode electrochemical cell, the same as that described in Section 2.5, was connected with the pumping system. 1 M Na_2CO_3 was used as the background electrolyte. The linear voltammetry technique was employed with a constant scan rate of 0.005 V/s. The applied potential ranges were from 0.2 to -1.2 and from 0.2 to 0.8 V, for the determinations of ferricyanide and ferrocyanide concentrations, respectively. The limiting currents on the current plateaus (about -0.6 to -0.2 V for ferricyanide and 0.4–0.6 V for ferrocyanide) were used to determine the concentrations of ferricyanide and ferrocyanide. The measurement noise was significantly increased when the pumping system was introduced. The function 'SG smooth' in the software Autolab Nova 1.10 was used to automatically minimise the detection noise. The detection sensitivity and LOD were determined by the same procedures described in Section 2.5.

3. Results and discussion

3.1. Fluid permeability, surface area and electrochemical properties of porous Ni electrode

Fig. 2a shows the porous structure of the LCS porous Ni sample at a low magnification. The pores are negative replicas of the K_2CO_3 particles and are interconnected with each other, making the porous Ni highly permeable. Fig. 2c shows the length-normalised pressure drop as a function of Darcian velocity of the LCS porous Ni. By fitting the plot to Eq. (1), the fluid permeability of the sample was determined as 1.50×10^{-10} m^2, which agrees with recent work on the fluid permeability of porous metals manufactured by powder metallurgy based methods [31,32]. High fluid permeability is a prerequisite for the porous Ni to be a successful electrode for limiting current sensors, as the solution is forced to flow through the working electrode during detection. The porous Ni sample is intact under the high pressure, up to 2 MPa/m, exerted by the flowing fluid during the test, indicating that the LCS porous Ni has a robust porous structure.

Fig. 2b shows the microstructure of the LCS porous Ni at a higher magnification. The Ni particles are visible and are partially sintered together with numerous interstices between adjacent particles, providing a high surface area. Fig. 2d presents the nitrogen adsorption isotherm of the porous Ni sample. The BET surface area was calculated by the BET model using data in the relative pressure (P/P_0) range of 0.05–0.3 [33], as shown in the inset of Fig. 2d. The gravimetric BET surface area of the porous Ni sample is 0.67 m^2/g, which is more than 20 times higher than that of electrodeposited porous Ni [34]. The high surface area is beneficial for improving the reaction rate and in turn detection performance. It should be

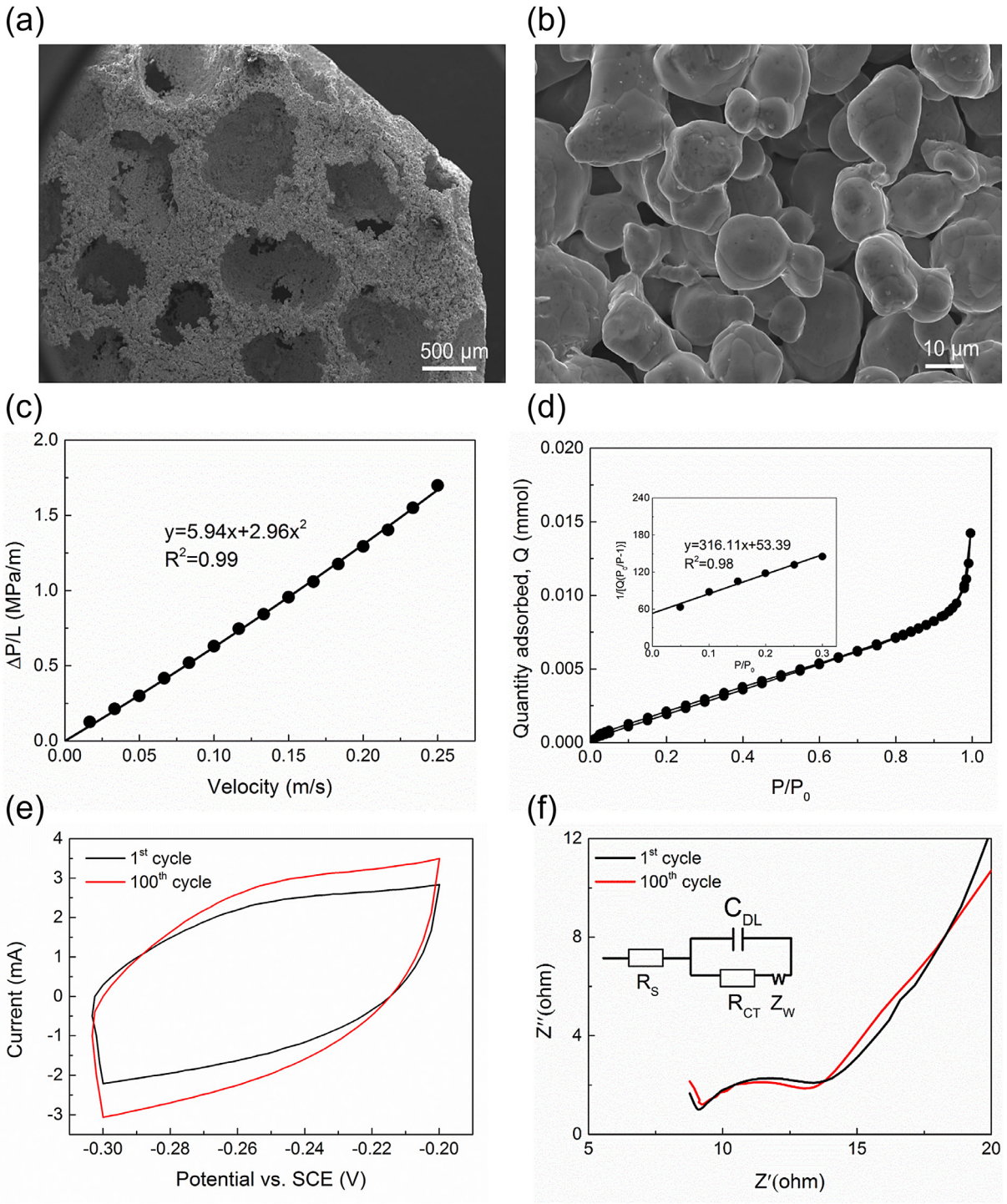

Fig. 2. SEM images of the porous Ni electrode taken at low (a) and high (b) magnifications; fluid permeability (c), BET surface area (d), double layer capacitance (e) and electrochemical impedance (f) measurements of the LCS porous Ni.

noted that both permeability and surface area of the LCS porous Ni vary markedly with porosity [35–37]. With increasing porosity, the volumetric BET surface area decreases but the permeability increases (Fig. S1). Besides, the mass transfer coefficient also decreases with increasing porosity [38]. Given that the LCS process can produce porous metals with a wide porosity range from 0.5 to 0.85, a medium porosity of 0.7 was therefore chosed for a trade-off between the BET surface area, permeability and mass transfer properties.

Fig. 2e and f also show that the LCS porous Ni sample has a gravimetric double layer capacitance around 10 mF/g and a charge transfer resistance of about 7 Ω. Both the double layer capacitance and charge transfer resistance of the LCS porous Ni sample are stable in 100 cycles.

In all, the high fluid permeability, robust structure, high surface area and good electrochemical properties make the LCS porous Ni an ideal electrode for the limiting current sensor.

3.2. Conventional electrochemical sensor

Fig. 3 shows the characteristics of the conventional electrochemical sensor in the detection of ferricyanide and ferrocyanide.

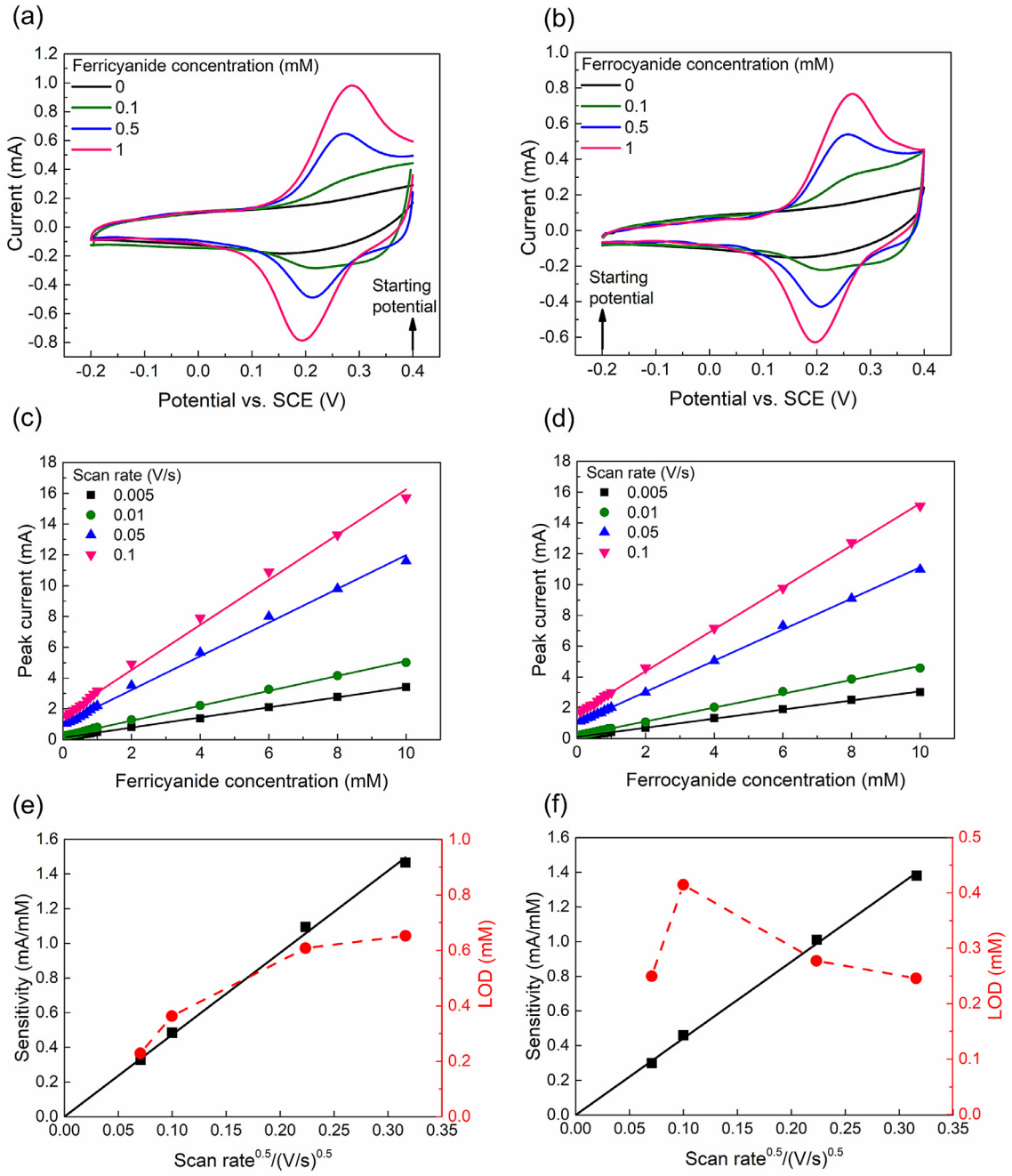

Fig. 3. Voltammograms for the detection of ferricyanide (a) and ferrocyanide (b) obtained at a scan rate of 0.01 V/s; relations between peak current and ferricyanide (c) and ferrocyanide (d) concentration at different scan rates; detection sensitivity and LOD against the square root of scan rate for ferricyanide (e) and ferrocyanide (f).

Fig. 3a and b show the voltammograms of ferricyanide and ferrocyanide, respectively, at different concentrations and at an identical scan rate of 0.01 V/s. When the concentration of ferricyanide or ferrocyanide is zero (black), there is no current peak. As the concentration of ferricyanide or ferrocyanide increases from 0 to 0.1, 0.5 and further to 1 mM, anodic and cathodic peak currents can be clearly observed at a potential of about 0.25 and 0.2 V, respectively. The peak currents increase with increasing concentration. As the redox reaction between ferrocyanide and ferrocyanide is a quasi-reversible process [15,39], the magnitude of the anodic peak current is very close to that of the cathodic peak current. The anodic peak current was used as the detection signal because it is easier to take readings from the anodic peak than from the cathodic peak.

Fig. 3c and d show the relations between the anodic peak current and the ferricyanide or ferrocyanide concentration, respectively. The anodic peak current increases linearly with the concentration in the range of 0.1–10 mM. Concentrations higher than 10 mM lead to high peak currents and serious solution IR drops, resulting in serious distortions in the voltammograms (Fig. S2). The detection sensitivity is equal to the slope of the fitted lines. The detection sensitivities for ferricyanide and ferrocyanide at scan rates of 0.005, 0.01, 0.05, 0.1 V/s are 0.33 and 0.30, 0.48 and 0.45, 1.09 and 1.01, 1.47 and 1.36 mA/mL, respectively.

Fig. 3e and f show that the sensitivity is proportional to the square root of scan rate, confirming that the redox reaction between ferricyanide and ferrocyanide is diffusion-controlled [40]. This is because the peak current is proportional to the square

root of scan rate at a fixed concentration, so does the sensitivity. It should be noted that the sensitivity for ferricyanide detection is slightly higher than for ferrocyanide detection. This is probably because ferricyanide has a higher diffusion coefficient than ferrocyanide [41].

The LOD of the conventional electrochemical sensor is influenced by the detection range and scan rate. For the full range detection from 0.1 to 10 mM, the LODs for ferricyanide and ferrocyanide are 0.23 and 0.25 mM (0.005 V/s), 0.36 and 0.42 mM (0.01 V/s), 0.61 and 0.28 mM (0.05 V/s), 0.65 and 0.25 mM (0.1 V/s), respectively. If we narrow the detection range to 0.1 – 1 mM, the LODs are reduced to 0.08 and 0.10 mM (0.005 V/s), 0.08 and 0.06 mM (0.01 V/s), 0.10 and 0.07 mM (0.05 V/s), 0.10 and 0.09 mM (0.1 V/s) (see Figs. S3 and S4). It is worth mentioning that the detection sensitivities obtained in the small detection range of 0.1–1 mM (Figs. S3b and S4b) are also slightly different from that obtained in the full detection range of 0.1–10 mM (Fig. 3e and f). In practical applications, different detection modes can be adopted in different detection ranges to achieve better accuracy. The LODs at different scan rates can be seen from Fig. 3e and f (as well as Figs. S3b and S4b). The effect of scan rate on the LOD is twofold. A high scan rate leads to a high peak current and therefore high detection sensitivity. On the one hand, increasing scan rate tends to lower LOD, because LOD is inversely proportional to detection sensitivity (Eq. (3)). On the other hand, a high peak current obtained at a high scan rate can result in a large IR drop and serious distortion in the voltammogram, increasing 'detection noise' and in turn LOD. The overall effect of scan rate on the LOD, however, is not pronounced.

3.3. Limiting current sensor

Fig. 4 shows the characteristics of the limiting current sensor in the detection of ferricyanide and ferrocyanide. Fig. 4a and b display the current-potential plots of ferricyanide and ferrocyanide, respectively, at different concentrations and at an identical flow rate of 16.8 mL/min. The limiting current is determined by the current plateau in the current-potential plot, which is controlled by the mass transfer rate of the analyte [42]. When there is no ferricyanide or ferrocyanide, the limiting current is about zero. As the concentration of ferricyanide or ferrocyanide increases, the limiting current moves negatively or positively, respectively. Fig. 4c and d show the relations between the limiting current and the concentration at three different flow rates of 16.8, 42 and 84 mL/min. The limiting current increases linearly with the concentration in the range from 0.005 to 1 mM. Concentrations higher than 1 mM result in high limiting currents and therefore serious distortion in the current-potential plots (see Fig. S5). The detection sensitivity of the limiting current sensor is determined by the slope of the fitted lines in Fig. 4c and d, following the same procedure as for the conventional electrochemical sensor. The sensitivities for the detection of ferricyanide and ferrocyanide at flow rates of 16.8, 42, 84 mL/min are 7.36 and 7.21, 13.79 and 12.48, 20.13 and 20.24 mA/mM, respectively. The sensitivity increases significantly with increasing flow rate. Fig. 4e and f plot the sensitivity against the mass transfer coefficient at different flow rates. The mass transfer coefficient of the LCS porous Ni was taken from our previously published work [38]. It can be seen that the detection sensitivities for ferricyanide and ferrocyanide are proportional to the mass transfer coefficient. The enhancement in sensitivity at a high flow rate can therefore be attributed to the enhanced mass transfer rate.

The LOD of the limiting current sensor varies significantly with the detection range. In a wide concentration range from 0.003 to 1 mM, the LODs for ferricyanide and ferrocyanide at flow rates of 16.8, 42, 84 mL/min are 13.55 and 13.69 μM, 28.60 and 21.50 μM, 17.05 and 21.91 μM, respectively (Fig. 3e and f). When the concentration is confined in a small range of 0.003 – 0.01 mM, the corresponding LODs are as low as 0.86 and 0.51 μM, 0.85 and 0.39 μM, 0.78 and 0.56 μM, respectively (Fig. S6). Similar to the effects of scan rate, the flow rate (or mass transfer rate) has both positive and negative effects on the LOD. The overall effect is not pronounced (Figs. 4e and f, S6).

3.4. Enhanced performance of limiting current sensor

Table 1 compares the detection performance between the limiting current sensor and the conventional electrochemical sensor. The limiting current sensor has sensitivities in the ranges of 7.36–20.13 and 7.21–20.24 mA/mM and LODs in the ranges of 0.78–0.86 and 0.39–0.56 μM, for the detection of ferricyanide and ferrocyanide, respectively. The conventional electrochemical sensor has corresponding sensitivities in the ranges of 0.33–1.47 and 0.30–1.36 mA/mM and LODs in the ranges of 75.53–101.81 and 64.19–101.52 μM. Comparing the average values of these two sensors shows that the limiting current sensor exhibits more than 10 times higher sensitivities and 100 times lower LODs than the conventional electrochemical sensor.

The enhanced performance of the limiting current sensor can be attributed to the introduction of the pumping system, which increases mass transfer and consequently increases the electrochemical reaction rate, as both sensors use the same porous Ni working electrode and utilise the same redox reaction. For the conventional electrochemical sensor, the detection is conducted in a static state and the reaction rate is limited by the diffusion of the reactive species [43]. In contrast, the limiting current sensor detects ferricyanide and ferrocyanide in a dynamic state. The reaction rate is controlled by the mass transfer process which includes not only diffusion but also convection [38]. The porous structure causes turbulent flow as the solution passes through the porous electrode, especially at high flow rates [44], speeding up mass transfer markedly [38]. Therefore, the reaction rate and detection performance are greatly improved. Taking the reduction reaction of 1 mM ferricyanide as an example, the maximum peak current is around 3 mA (Fig. 3c) while the maximum limiting current is more than 20 mA (Fig. 4c), indicating that the convection is the dominant mode for mass transportation in the limiting current sensor. The introduction of the pumping system inevitably increases the detection noise of the sensor. However, the noise can be minimised by software. The residual standard deviation of the best-fit regression line between peak/limiting current and ion concentration, σ, can be regarded as an indicator of the noise. In the entire concentration ranges, the values of σ for the conventional sensor (Fig. 3c and d) and the limiting current sensor (Fig. 4c and d) are in the ranges of 0.02–1.1 and 0.02–1.4, respectively, indicating very similar levels of noise. It confirms that the noise arisen from the pumping system was effectively removed by the software and should not affect the detection significantly.

3.5. Thermal stability

Fig. 5 shows the variations of peak current and limiting current with ambient temperature. The peak current was measured by the conventional electrochemical sensor in 1 mM ferricyanide/ferrocyanide solution at a scan rate of 0.01 V/s. The limiting current was measured by the limiting current sensor with 0.1 mM ferricyanide/ferrocyanide solution at a flow rate of 16.8 mL/min. The peak current increases more significantly with rising temperature than the limiting current does. There is an increase of about 60% in peak current compared with an increase of about 10% in limiting current, when the temperature is increased from 25 to 55 °C, indicating that the limiting current sensor has

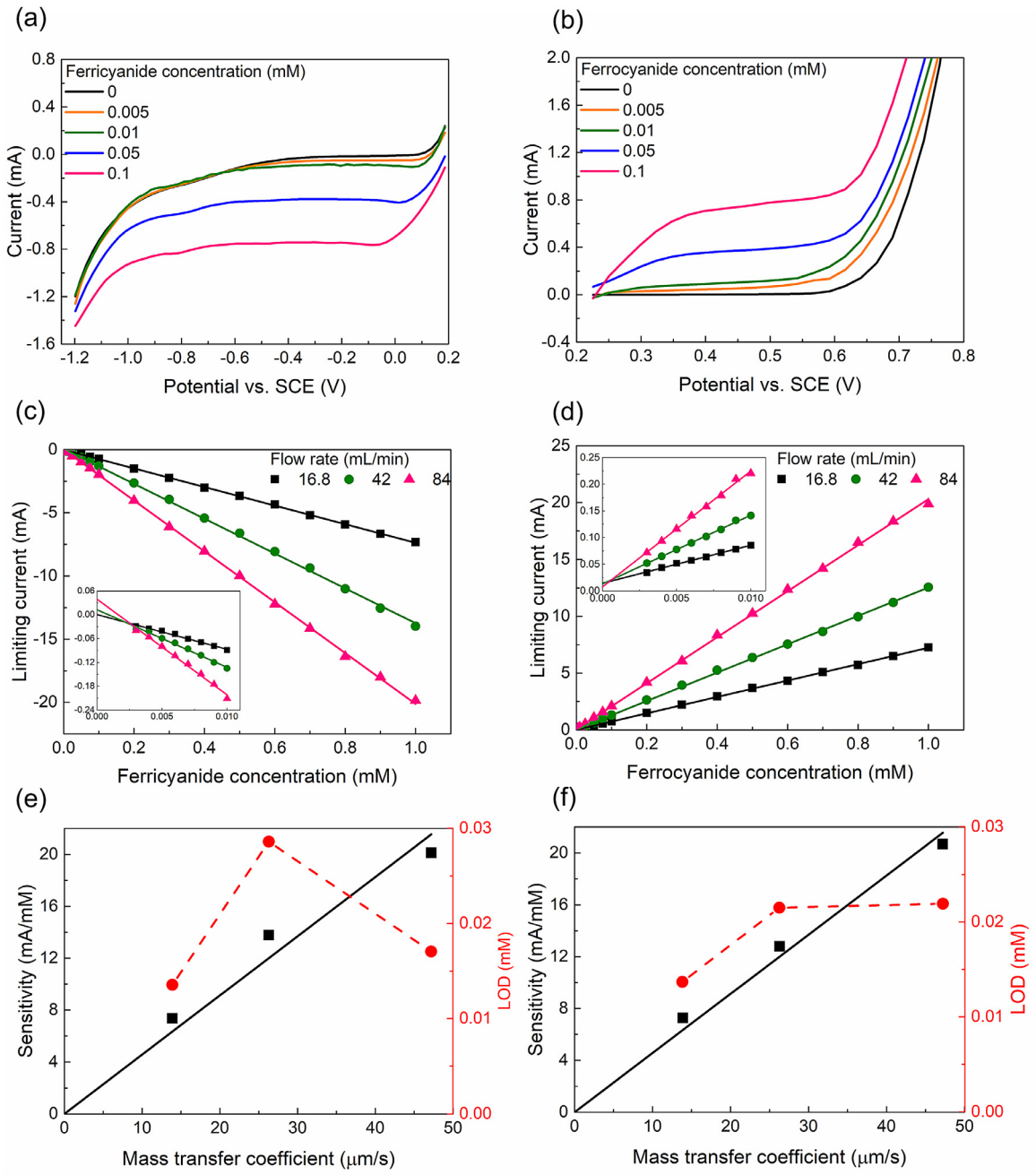

Fig. 4. Current-potential plots of the limiting current sensor for the detection of ferricyanide (a) and ferrocyanide (b), at a flow rate of 16.8 mL/min; relations between limiting current and ferricyanide (c) or ferrocyanide (d) concentration at different flow rates; detection sensitivity and LOD against the mass transfer coefficient for ferricyanide (e) and ferrocyanide (f).

Table 1
Detection performance of the limiting current sensor and the conventional electrochemical sensor.

Sensor	Flow rate (mL/min)	Scan rate (V/s)	Sensitivity (mA/mM)		LOD (μM)	
			Ferri-	Ferro-	Ferri-	Ferro-
Limiting current sensor	16.8	0.005	7.36	7.21	0.86	0.51
	42	0.005	13.79	12.48	0.85	0.39
	84	0.005	20.13	20.24	0.78	0.56
Conventional electrochemical sensor	–	0.005	0.33	0.30	75.53	101.52
	–	0.01	0.48	0.45	83.71	64.19
	–	0.05	1.09	1.01	101.81	66.47
	–	0.1	1.47	1.36	97.01	92.76

Note: (1) Ferri- and Ferro- stand for Ferricyanide and Ferrocyanide, respectively. (2) The LODs of the limiting current sensor and the conventional electrochemical sensor are determined in the concentration ranges of 0.003 – 0.01 and 0.1 – 1 mM, respectively.

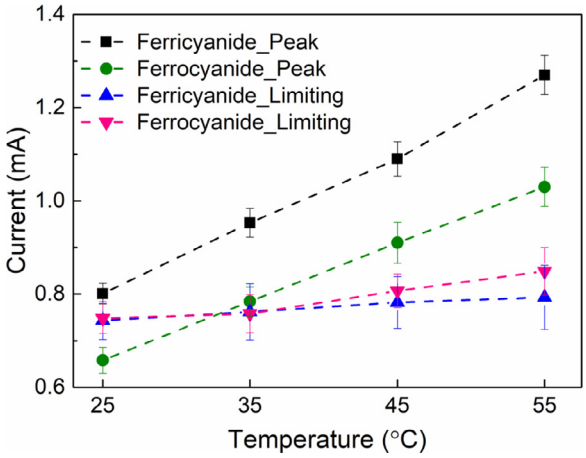

Fig. 5. Variations of peak current or limiting current with temperature. Peak currents were measured in 1 mM ferricyanide/ferrocyanide at a scan rate of 0.01 V/s, and limiting currents in 0.1 mM ferricyanide/ferrocyanide at a flow rate of 16.8 mL/min.

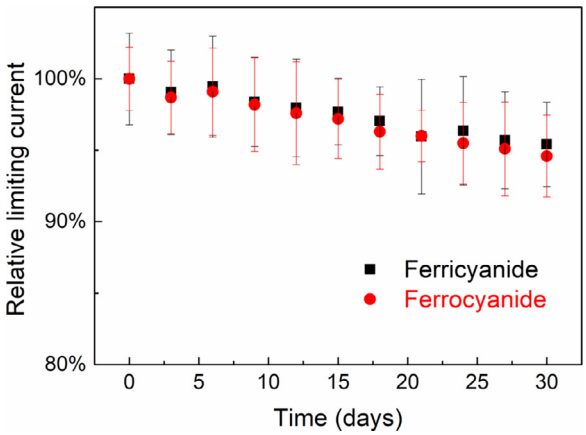

Fig. 6. Relative limiting current measured by the limiting current sensor in 0.1 mM ferrocyanide and ferricyanide at a flow rate of 16.8 mL/min and a temperature of 25 °C within 30 days.

better thermal stability than the conventional electrochemical sensor. As discussed in Section 3.4, the peak current is solely controlled by the diffusion of reactive species while the limiting current is mainly controlled by the convection of reactive species. The peak current is sensitive to temperature because the diffusion rates of ferricyanide and ferrocyanide increase markedly with increasing temperature [45]. The good thermal stability of the limiting current sensor implies that the convection within porous Ni is mainly dependant on flow regime rather than temperature. The limiting current sensor is advantageous in practical applications because the electrochemical detections can be conducted under different environmental conditions.

3.6. Long-term stability

Fig. 6 shows the relative limiting currents, i.e. the percentages relative to the initial limiting current, measured by the limiting current sensor every three days in 0.1 mM ferricyanide/ferrocyanide at a flow rate of 16.8 mL/min and at 25 °C. The limiting current has only a small drop of about 5% after 30 days for both ferricyanide and ferrocyanide detection. The excellent long-term stability of the LCS porous Ni electrode is derived from its electrochemical stability and robust structure. Porous Ni has excellent electrochemical stability and provides stable performance for sensing ferricyanide and ferrocyanide over a long working time, as evidenced in Fig. 2e and f. The LCS porous Ni sample has a porosity of 0.7, which leads to a good balance between mechanical strength and fluid permeability. Higher porosities can result in lower mechanical strengths [25], which may not be able to withstand the high pressure of the flowing solution for a long period of time. Lower porosities can lead to low fluid permeability which may compromise the detection performance.

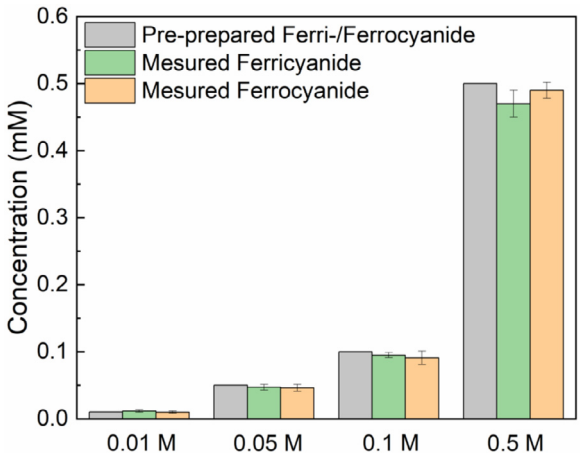

Fig. 7. Detection of ferricyanide and ferrocyanide in tap water based solutions by the limiting current sensor at a flow rate of 16.8 mL/min.

3.7. Selectivity in tap water based solutions

To test the selectivity of the limiting current sensor for ferricyanide and ferrocyanide detection in the presence of other ions, we prepared aqueous solutions using tap water with known ferricyanide/ferrocyanide additions to give pre-prepared concentrations of 0.01, 0.05, 0.1 and 0.5 mM. 1 M Na_2CO_3 was added to increase the conductivity of the tap water. These tap water solutions were then forced to flow through the limiting current sensor at a flow rate of 16.8 mL/min. The measured concentrations of ferricyanide and ferrocyanide in tap water were calculated by the limiting current, according to the quantitative relations obtained from Fig. 4c and d. Fig. 7 shows that the measured concentrations are very close to the pre-prepared concentrations, indicating that the limiting current sensor has good selectivity in tap water. The main ions existing in the tap water in the Northwest of England are SO_4^{2-}, Cl^{-1}, Na^+, Ca^{2+}, etc. (Table S1). The presence of these ions in tap water does not interfere with the detection performance of the limiting current sensor for ferricyanide and ferrocyanide.

3.8. Comparison with other sensors

Table 2 compares the performance of various sensors for the detection of ferricyanide and ferrocyanide. The limiting current sensor developed in this work has a sensitivity two orders of magnitude higher than the conventional electrochemical sensors reported by Pandurangachar et al. [19] and Niranjana et al. [24], which used surface-modified carbon paste working electrode. The amperometric sensitivity is not applicable for the spectroelectrochemical sensors as they detect ferricyanide/ferricyanide by the light absorbence of the electrode. The LOD of the limiting current sensor is one order of magnitude lower than that of the spectroelectrochemical sensors [21,23] and two orders of magnitude lower than that of the conventional electrochemical sensors in the literature [19,24]. Compared with the conventional electrochemical sensors with surface-modified carbon paste working electrode, the conventional electrochemical sensor in this work shows a lower

Table 2
Comparison of various sensors for the detection of ferricyanide and ferrocyanide.

Sensor	Sensitivity (mA/mM)	LOD (μM)	Linear Range (μM)	Reference
Limiting current sensor (Ferri- and Ferro-)	7.21–20.24	0.4	3–1000	This work
Conventional electrochemical sensor (Ferri- and Ferro-)	0.30–1.47	64	100–10,000	This work
Conventional electrochemical sensor (Ferri- only)	0.012	100	500–3000	[19]
Conventional electrochemical sensor (Ferri- only)	0.0233	100	1000–3000	[24]
Spectroelectrochemical sensor (Ferri- only)	–	8	8–50	[21]
Spectroelectrochemical sensor (Ferro- only)	–	50	50–5000	[23]

Note: The detection sensitivities and LODs of the limiting current sensor and conventional electrochemical sensor apply to both ferricyanide and ferrocyanide.

LOD and a more than 10 times higher sensitivity, attributable to the high surface area and excellent electrochemical properties of the porous Ni electrode. Overall, the superior detection performance of the limiting current sensor is derived from combining the novel design of a dynamic sensor with a porous working electrode.

The detection range of the limiting current sensor is 3–1000 μM, which is relatively small. For the pursuit of ultralow detection limit, the detection range sometimes needs to be further reduced to 3–10 μM. Another limitation of the limiting current sensor is that it requires a vast amount of solution and a longer response time than the conventional electrochemical and spectroelectrochemical sensors. These issues can be solved by the miniaturization of the sensor prototype and porous electrode using emerging microfabrication and microfluidics techniques.

4. Conclusions

A limiting current sensor prototype has been developed for the detection of ferricyanide and ferrocyanide. The limiting current sensor consists of a three-electrode electrochemical cell equipped with a porous Ni working electrode and a pumping system. The pumping system forces the solution to pass through the porous Ni electrode, increasing the mass transfer rate markedly. The enhanced mass transfer rate, together with the high surface area of the porous Ni electrode, increases the reaction rate and gives rise to the superior detection performance of the limiting current sensor. The limiting current sensor shows a sensitivity of 7.21–20.24 mA/mM and a LOD of 0.4 μM, which are two orders of magnitude higher and one order of magnitude lower, respectively, than previously reported sensors. Moreover, the limiting current sensor exhibits excellent thermal stability in a temperature range of 25–55 °C, good long-term stability after 30 days and good selectivity against interfering ions in tap water.

Declaration of Competing Interest

The authors have declared no conflict of interest.

Credit authorship contribution statement

Pengcheng Zhu: Conceptualization, Investigation, Writing – original draft, Writing – review & editing. **Yuyuan Zhao:** Conceptualization, Writing – review & editing, Funding acquisition, Project administration.

Acknowledgement

This work was supported by an IAA award as further funding from the Engineering and Physical Sciences Research Council (Grant No. EP/N006550/1).

Supplementary materials

Supplementary material associated with this article can be found, in the online version, at doi:10.1016/j.electacta.2021.138428.

References

[1] L. Huang, S. Tian, W. Zhao, K. Liu, J. Guo, Electrochemical vitamin sensors: a critical review, Talanta 222 (2020) 121645.
[2] E. Bakker, M. Telting-Diaz, Electrochemical sensors, Anal. Chem. 74 (2002) 2781–2800.
[3] E. Sehit, Z. Altintas, Significance of nanomaterials in electrochemical glucose sensors: an updated review (2016–2020), Biosens. Bioelectron. (2020) 112165.
[4] A.A. Lahcen, S. Rauf, T. Beduk, C. Durmus, A. Aljedaibi, S. Timur, H.N. Alshareef, A. Amine, O.S. Wolfbeis, K.N. Salama, Electrochemical sensors and biosensors using laser-derived graphene: a comprehensive review, Biosens. Bioelectron. (2020) 112565.
[5] Y. Si, H.J. Lee, Carbon nanomaterials and metallic nanoparticles-incorporated electrochemical sensors for small metabolites: detection methodologies and applications, Curr. Opin. Electrochem. (2020).
[6] G. Hanrahan, D.G. Patil, J. Wang, Electrochemical sensors for environmental monitoring: design, development and applications, J. Environ. Monit. 6 (2004) 657–664.
[7] B. Bansod, T. Kumar, R. Thakur, S. Rana, I. Singh, A review on various electrochemical techniques for heavy metal ions detection with different sensing platforms, Biosens. Bioelectron. 94 (2017) 443–455.
[8] X. Sun, F. Liu, C. Wang, X. Liu, J. Jian, D. Zeng, L. Liu, H. Yuan, G. Lu, A dense diffusion barrier limiting current oxygen sensor for detecting full concentration range, Sens. Actuators B Chem. 305 (2020) 127521.
[9] T. Liu, X. Wang, X. Zhang, X. Gao, L. Li, J. Yu, X. Yin, A limiting current oxygen sensor prepared by a co-pressing and co-sintering technique, Sens. Actuators B Chem. 277 (2018) 216–223.
[10] C. Wang, T. Liu, X. Wang, J. Li, H. Jin, J. Yu, M. Yi, Y. Mo, A novel limiting current oxygen sensor prepared by slurry spin coating, Sens. Actuators B Chem. 270 (2018) 518–524.
[11] S. Akasaka, Y. Amamoto, H. Yuji, I. Kanno, Limiting current type yttria-stabilized zirconia thin-film oxygen sensor with spiral Ta_2O_5 gas diffusion layer, Sens. Actuators B Chem. (2020) 128932.
[12] G.D. Lawrence, S. Fishelson, Blueprint photography by the cyanotype process, J. Chem. Educ. 76 (1999) 1216A.
[13] M. Na, Y. Chen, Y. Han, S. Ma, J. Liu, X. Chen, Determination of potassium ferrocyanide in table salt and salted food using a water-soluble fluorescent silicon quantum dots, Food Chemistry 288 (2019) 248–255.
[14] P.A. Haas, A review of information on ferrocyanide solids for removal of cesium from solutions, Sep. Sci. Technol. 28 (1993) 2479–2506.
[15] J. Luo, A. Sam, B. Hu, C. DeBruler, X. Wei, W. Wang, T.L. Liu, Unraveling pH dependent cycling stability of ferricyanide/ferrocyanide in redox flow batteries, Nano Energy 42 (2017) 215–221.
[16] D.R. Lide, CRC Handbook of Chemistry and Physics, CRC Press, 2004.
[17] R. Ojani, E. Ahmadi, J.-.B. Raoof, F. Mohamadnia, Characterization of a carbon paste electrode containing organically modified nanostructure silica: application to voltammetric detection of ferricyanide, J. Electroanal. Chem. 626 (2009) 23–29.
[18] I. Taurino, S. Carrara, M. Giorcelli, A. Tagliaferro, G. De Micheli, Comparison of two different carbon nanotube-based surfaces with respect to potassium ferricyanide electrochemistry, Surf. Sci. 606 (2012) 156–160.
[19] M. Pandurangachar, B.K. Swamy, B. Chandrashekar, O. Gilbert, S. Reddy, B. Sherigara, Electrochemical investigations of potassium ferricyanide and dopamine by 1-butyl-4-methylpyridinium tetrafluoro borate modified carbon paste electrode: a cyclic voltammetric study, Int. J. Electrochem. Sci. 5 (2010) 1187–1202.
[20] W.R. Heinema, C.J. Seliskar, J.N. Richardson, Spectroelectrochemical sensing based on multimode selectivity simultaneously achievable in a single device: an overview, Aust. J. Chem. 56 (2003) 93–102.
[21] Y. Shi, A.F. Slaterbeck, C.J. Seliskar, W.R. Heineman, Spectroelectrochemical sensing based on multimode selectivity simultaneously achievable in a single device. 1. Demonstration of concept with ferricyanide, Anal. Chem. 69 (1997) 3679–3686.

[22] M. Maizels, C.J. Seliskar, W.R. Heineman, S.A. Bryan, Spectroelectrochemical sensing based on multimode selectivity simultaneously achievable in a single device. 10. Sensing of ferrocyanide in hanford tank waste simulant solution, Electroanal. Int. J. Devot. Fundam. Pract. Asp. Electroanal. 14 (2002) 1345–1352.
[23] M.L. Stegemiller, W.R. Heineman, C.J. Seliskar, T.H. Ridgway, S.A. Bryan, T. Hubler, R.L. Sell, Spectroelectrochemical sensing based on multimode selectivity simultaneously achievable in a single device. 11. Design and evaluation of a small portable sensor for the determination of ferrocyanide in hanford waste samples, Environ. Sci. Technol. 37 (2003) 123–130.
[24] E. Niranjana, B.K. Swamy, R.R. Naik, B. Sherigara, H. Jayadevappa, Electrochemical investigations of potassium ferricyanide and dopamine by sodium dodecyl sulphate modified carbon paste electrode: a cyclic voltammetric study, J. Electroanal. Chem. 631 (2009) 1–9.
[25] Y. Zhao, T. Fung, L. Zhang, F. Zhang, Lost carbonate sintering process for manufacturing metal foams, Scr. Mater. 52 (2005) 295–298.
[26] Z. Xiao, Y. Zhao, Heat transfer coefficient of porous copper with homogeneous and hybrid structures in active cooling, J. Mater. Res. 28 (2013) 2545–2553.
[27] E. Moreira, M. Innocentini, J. Coury, Permeability of ceramic foams to compressible and incompressible flow, J. Eur. Ceram. Soc. 24 (2004) 3209–3218.
[28] J.J. Van Benschoten, J.Y. Lewis, W.R. Heineman, D.A. Roston, P.T. Kissinger, Cyclic voltammetry experiment, J. Chem. Educ. 60 (1983) 772.
[29] U. Guth, W. Vonau, J. Zosel, Recent developments in electrochemical sensor application and technology-a review, Meas. Sci. Technol. 20 (2009) 042002.
[30] A. Shrivastava, V. Gupta, Methods for the determination of limit of detection and limit of quantitation of the analytical methods, Chron. Young Sci. 2 (2011) 21-21.
[31] J.F. Despois, A. Mortensen, Permeability of open-pore microcellular materials, Acta Mater. 53 (2005) 1381–1388.
[32] A. Otaru, A.R. Kennedy, The permeability of virtual macroporous structures generated by sphere packing models: comparison with analytical models, Scripta Mater. 124 (2016) 30–33.
[33] M. Thommes, K. Kaneko, A.V. Neimark, J.P. Olivier, F. Rodriguez-Reinoso, J. Rouquerol, K.S. Sing, Physisorption of gases, with special reference to the evaluation of surface area and pore size distribution (IUPAC technical report), Pure Appl. Chem. 87 (2015) 1051–1069.
[34] F. Bidault, D.J.L. Brett, P.H. Middleton, N. Abson, N.P. Brandon, A new application for nickel foam in alkaline fuel cells, Int. J. Hydrogen Energy 34 (2009) 6799–6808.
[35] P. Zhu, Y. Zhao, Effects of electrochemical reaction and surface morphology on electroactive surface area of porous copper manufactured by lost carbonate sintering, RSC Adv. 7 (2017) 26392–26400.
[36] P. Zhu, Z. Wu, Y. Zhao, Hierarchical porous Cu with high surface area and fluid permeability, Scr. Mater. 172 (2019) 119–124.
[37] P. Zhu, Y. Zhao, Cyclic voltammetry measurements of electroactive surface area of porous nickel: peak current and peak charge methods and diffusion layer effect, Mater. Chem. Phys. 233 (2019) 60–67.
[38] P. Zhu, Y. Zhao, Mass transfer performance of porous nickel manufactured by lost carbonate sintering process, Adv. Eng. Mater. 19 (2017) 1700392.
[39] A. Khoshroo, K. Sadrjavadi, M. Taran, A. Fattahi, Electrochemical system designed on a copper tape platform as a nonenzymatic glucose sensor, Sens. Actuators B Chem. 325 (2020) 128778.
[40] A.T. Valota, P.S. Toth, Y.-J. Kim, B.H. Hong, I.A. Kinloch, K.S. Novoselov, E.W. Hill, R.A. Dryfe, Electrochemical investigation of chemical vapour deposition monolayer and bilayer graphene on the microscale, Electrochim. Acta 110 (2013) 9–15.
[41] S. Konopka, B. McDuffie, Diffusion coefficients of ferri-and ferrocyanide ions in aqueous media, using twin-electrode thin-layer electrochemistry, Anal. Chem. 42 (1970) 1741–1746.
[42] F. Recio, P. Herrasti, L. Vazquez, C.P. de León, F. Walsh, Mass transfer to a nanostructured nickel electrodeposit of high surface area in a rectangular flow channel, Electrochim. Acta 90 (2013) 507–513.
[43] R.E. Smith, T.J. Davies, N.d.B. Baynes, R.J. Nichols, The electrochemical characterisation of graphite felts, J. Electroanal. Chem. 747 (2015) 29–38.
[44] X. Lu, Y. Zhao, D.J. Dennis, Flow measurements in microporous media using micro-particle image velocimetry, Phys. Rev. Fluids 3 (2018) 104202.
[45] K. Ngamchuea, S. Eloul, K. Tschulik, R.G. Compton, Planar diffusion to macro disc electrodes-what electrode size is required for the cottrell and randles–sevcik equations to apply quantitatively? J. Solid State Electrochem. 18 (2014) 3251–3257.